

# The Watershed Line of the Distal Radius: Cadaveric and Imaging Study of Anatomical Landmarks

Minke Bergsma, MD<sup>1,2,3</sup>  Job N. Doornberg, MD, PhD<sup>1,2</sup> Annelise Borghorst, MD<sup>1</sup>  
W.A. Kernkamp, MD<sup>4,5</sup> R. L. Jaarsma, MD, PhD<sup>1</sup> Gregory I. Bain, MBBS, PhD<sup>1</sup>

<sup>1</sup> Department of Orthopaedic Surgery, Flinders Medical Centre/  
Department of Orthopaedic Trauma Surgery and the Biomechanics &  
Implants Research Group, Flinders University, Adelaide, Australia

<sup>2</sup> Department of Orthopaedic Surgery, Amsterdam University Medical  
Center/University of Amsterdam, Amsterdam, the Netherlands

<sup>3</sup> Department of Radiology, Noordwest Ziekenhuisgroep Alkmaar,  
Alkmaar, the Netherlands

<sup>4</sup> Department of General Surgery, Albert Schweizer Hospital,  
Dordrecht, the Netherlands

<sup>5</sup> Postdoctoral Research Fellowship, Shanghai Jiao Tong University,  
Shanghai, People's Republic of China

Address for correspondence Minke Bergsma, MD, Department of  
Radiology, Noordwest Ziekenhuisgroep, Postbus 501, 1800 AM  
Alkmaar, the Netherlands (e-mail: m.bergsma@nwz.nl).

J Wrist Surg 2020;9:44–51.

## Abstract

**Background** Placement of volar plates remains a challenge as the watershed line may not be an easy-identifiable distinct line intraoperatively.

**Objectives** The main objective of this article is to define how anatomical landmarks identifiable upon the volar surgical approach to the distal radius relate to the watershed line.

**Methods** We identified anatomical landmarks macroscopically upon standard volar approach to the distal radius in 10 cadaveric forearms and marked these with radiostereometric analysis (RSA) beads in cadaveric wrists. The RSA beads were then referenced against the volar osseous structures using quantification of three-dimensional computed tomography and advanced imaging software.

**Results** The mean measurements were the radial and ulnar prominences 11.1 mm and 2.1 mm proximal to the joint line of the distal radius, respectively. The interfossa sulcus was 0.3 mm proximal and 3 mm dorsal to the ulnar prominence. The watershed line was between 3.5 (minimal) and 7.6 (maximal) mm distal to the distal line of insertion of the pronator quadratus.

**Conclusion** The watershed line is situated distal to the pronator quadratus, but with a wide variability making it an impractical landmark for plate position. The osseous ulnar prominence is a good anatomical reference for safe plate positioning, as it is located on the watershed line and easily palpated at surgery. One should keep in mind the sulcus—the point on the watershed line where the flexor pollicis longus runs—can be situated just proximal to the ulnar prominence.

**Clinical Relevance** To provide anatomical landmarks that are easy to identify upon surgical approach without the direct need for intraoperative imaging.

## Keywords

- ▶ distal radius fracture
- ▶ watershed line
- ▶ volar approach
- ▶ anatomy
- ▶ Q3DCT imaging
- ▶ volar plating

received  
April 23, 2019  
accepted  
September 5, 2019  
published online  
December 20, 2019

Copyright © 2020 by Thieme Medical  
Publishers, Inc., 333 Seventh Avenue,  
New York, NY 10001, USA.  
Tel: +1(212) 760-0888.

DOI <https://doi.org/10.1055/s-0039-1698452>.  
ISSN 2163-3916.

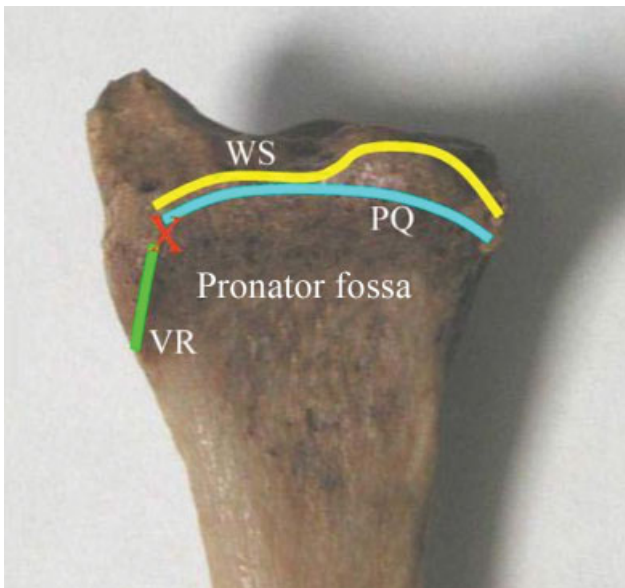


**Fig. 1** Nelson and Orbay coined the *watershed line* (WS) as “a theoretical line marking the most volar aspect of the volar margin of the radius,” to serve as the distal margin for volar plating to minimize tendon injuries.<sup>1–3</sup> PQ, pronator quadratus line, or PQ line; VR, volar radial ridge; WS, watershed line; X, volar radial tuberosity; (with permission from <http://eradius.com/AnatomyOfDistalRadius.htm><sup>3</sup>).

The watershed line should serve as the distal margin for the placement of a volar plate to minimize flexor tendon injuries. Orbay defined the watershed line as “a theoretical line marking the most volar aspect of the volar margin of the radius” (→ **Fig. 1**).<sup>1–3</sup> Flexor and extensor tendon irritation have been identified as the most frequent complication of internal fixation of unstable distal radius fracture with a volar locking-plate.<sup>4</sup> The majority of iatrogenic tendon complications include flexor tendons: ruptures of the flexor pollicis longus (FPL) tendon and flexor tendon tenosynovitis.<sup>4</sup> The clinical importance of the watershed line has been

described by Soong et al: plates prominent at the watershed line increase the risk of flexor tendon injury.<sup>5</sup> The authors advised surgeons to avoid implant prominence at the watershed line.<sup>5</sup>

The latter remains a challenge as cadaveric studies show that the watershed line may not be easy-identifiable intraoperatively.<sup>6,7</sup> As Imatani et al refer to their anatomical study, it may correspond to the distal margin of the pronator fossa in the radial half of the volar radius, and to a hypothetical line between the line that corresponds to the distal edge of the pronator fossa and a more prominent distal line in the ulnar half.<sup>6</sup> The ulnar prominence (or medial prominence as described by Imatani et al) on the volar radius is a recommended key structures for accurate plate placement to avoid flexor tendon injury.<sup>6,8</sup> However, many subsequent definitions have been published (see review Interpretations of the term ‘Watershed Line’ used as reference for volar plating in this edition of *Journal of Wrist Surgery*). This review is now titled Interpretations of the term ‘Watershed Line’ used as reference for volar plating. Moreover, macroscopically upon surgical approach, the appearance and identification of these advised osseous landmarks, as well as on fluoroscopy intraoperatively, may not be as well-defined<sup>5</sup> as suggested by cadaveric studies using wide nonsurgical dissection on dried bones<sup>6,7</sup>

To the best of our knowledge, no cadaveric studies have correlated the surgically identifiable key volar references to the watershed line using advanced imaging techniques.

Therefore, the purpose of our study is to (1) identify these defined anatomical landmarks macroscopically upon standard volar approach to the distal radius and mark these with radiostereometric analysis (RSA) beads in cadaveric wrists, and then (2) subsequently reference the RSA-marked anatomical landmarks with key volar osseous references of the watershed line as defined by the use of quantification of three-dimensional computed tomography (Q3DCT) using advanced imaging software<sup>9–11</sup> (→ **Fig. 2B** and **C**). The clinical relevance is to provide surgeons with intraoperative macroscopic landmarks that assist in correct plate position.

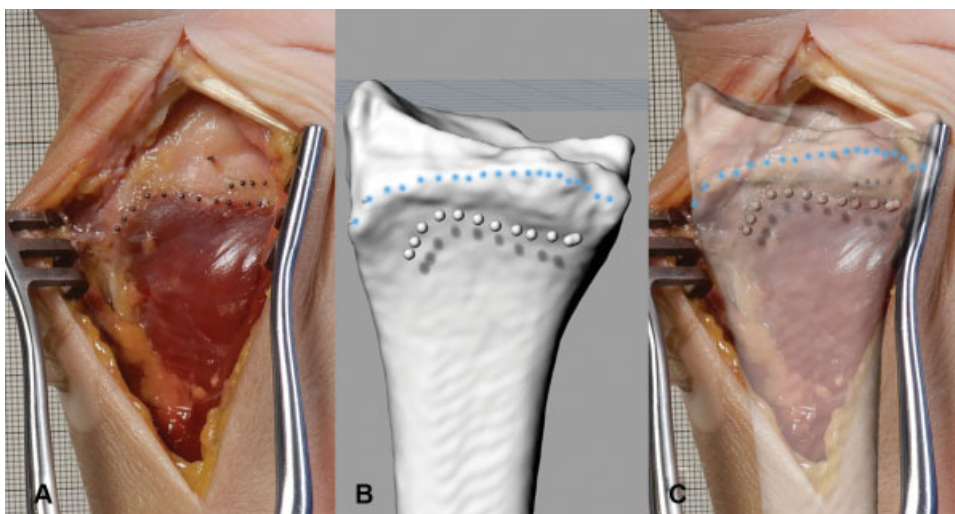


**Fig. 2** Anatomical landmarks of the volar cadaveric distal radius marked with radiostereometric analysis (RSA) beads (A). Cadaveric specimen with subsequent RSA-marked anatomical landmarks (B) was referenced using advanced imaging software (C)<sup>9–11</sup> with the volar osseous references of the watershed line (small dots).

## Materials and Methods

Our local Human Research Ethics Committee approved this study, in accordance with the Declaration of Helsinki, under protocol number 224.17.

### Cadaveric Specimens

This study was conducted with 10 left forearms including the elbow joint from fresh-frozen cadavers. These forearms were from six males and four females: mean age 65 (range: 42–90 years). None of the specimens had clinical or radiographic signs of prior surgery or trauma to the wrist.

### Soft Tissue Landmarks<sup>8,12–15</sup>: Soft Tissue Dissection and RSA Marking (→ Fig. 2)

The cadaveric wrist was positioned in supinated position to simulate the wrist during surgery in clinical practice. The forearm was secured on a wooden frame. The ulnar shaft, radial shaft, second, and fifth metacarpals were fixed with K-wires to a wooden frame to minimize movement during further study procedures. Onto a tripod, a camera was mounted (Canon, Coolpix, A900), and photographs were taken of the specimen throughout the study.

A volar flexor carpi radialis (FCR) approach<sup>16</sup> to the distal radius was performed, through the bed of the FCR sheath to the pronator quadratus (PQ) and the volar wrist capsule by the Orthopaedic Upper Limb and Trauma Fellow (JND). The flexor tendons were retracted—but not resected as in previous cadaveric studies to further mimic the volar approach to the radius in clinical practice.<sup>6</sup> The PQ muscle and capsular ligaments were not violated. Photographs of the specimens were obtained at this point using the mounted camera.

Twenty-one-gauge needles were placed in the distal radioulnar joint and in the radiocarpal joint. RSA marker beads were placed on the distal border of the PQ (→ Fig. 2A). The radial and ulnar osseous prominences on the volar aspect of the distal radius were palpated, and after consensus RSA

beads were secured on fibrous tissue overlying the maximal prominences. Photographs were repeated.

No further procedure to the distal radius was performed, and the PQ was not validated. The skin was sutured with Nylon (Ethicon, Ethilon, monofilament 3–0).

All specimens still fixed to the wooden frame underwent a CT scan using a GE Optima CT scanner (140 Kv, 200 mA, slice thickness 0.625 mm, interval 0.3 mm).

### Osseous Landmarks<sup>1–7,17–27</sup>: Watershed Line as Defined on Three-Dimensional Computed Tomography (→ Fig. 3)

The Digital Imaging and Communication in Medicine CT scans were loaded in 3D slicer (3D Slicer, Boston, MA). In 3D Slicer, osseous structures, including the pronator fossa, radial and ulnar osseous prominences defining the watershed line<sup>6</sup> and the interfossa sulcus for the FPL tendon, were segmented in axial, sagittal, and coronal planes. RSA beads marking (1) the distal border of the PQ and (2) the palpated radial and ulnar prominences were also segmented.

The watershed line was defined and segmented as the most volar aspects of the distal radius in each fifth sagittal image of 0.625 mm<sup>3</sup>. Separate Surface Tessellation Language (STL) files of the distal radius, (2) RSA markers and (3) the Watershed Line were created (→ Fig. 3). The segmentations were exported as 3D polygon mesh reconstructions.

The 3D polygon mesh reconstructions were subsequently imported into rhinoceros (McNeel, Seattle, WA) to quantify (1) the most prominent line of points of the volar aspect of the radius, (2) the radial and ulnar osseous prominences, and (3) distances between RSA soft tissue landmarks<sup>8,12–15</sup> and Q3DCT-defined osseous landmarks<sup>1–7,17–27</sup> (→ Fig. 3A). A coordinate system was created to standardize the axes and quantification of CT imaging for all specimens. The x-axis represented proximal to distal, the y-axis radioulnar, and the z-axis dorsal-to-volar. The x-axis representing the longitudinal axis of the radius was defined by the line through five

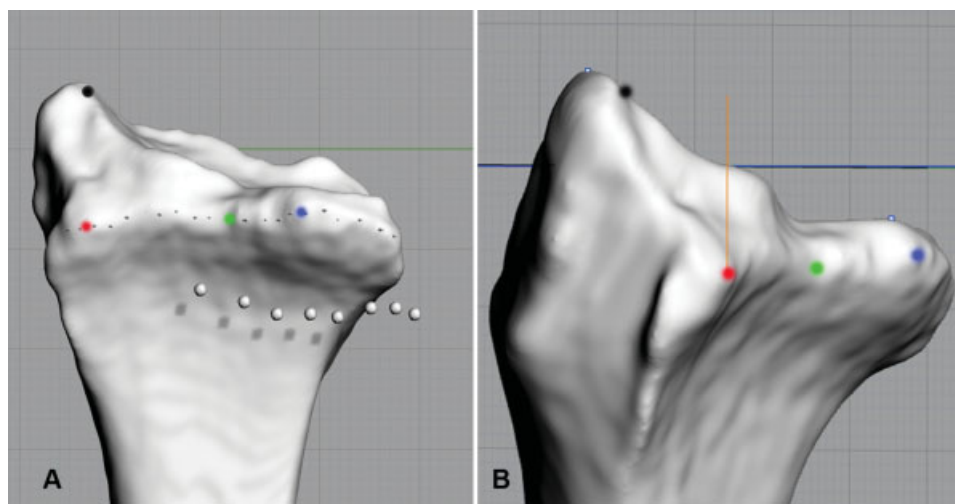


**Fig. 3** Three-dimensional polygon mesh reconstructions of the radius. (A) The most volar aspect of the radius (small dots) and the radial and ulnar osseous prominences (dark vague dots), and interfossa sulcus (light vague dot) are marked. In (B) the vertical line shows proximal–distal measurements performed parallel to the x-axis.

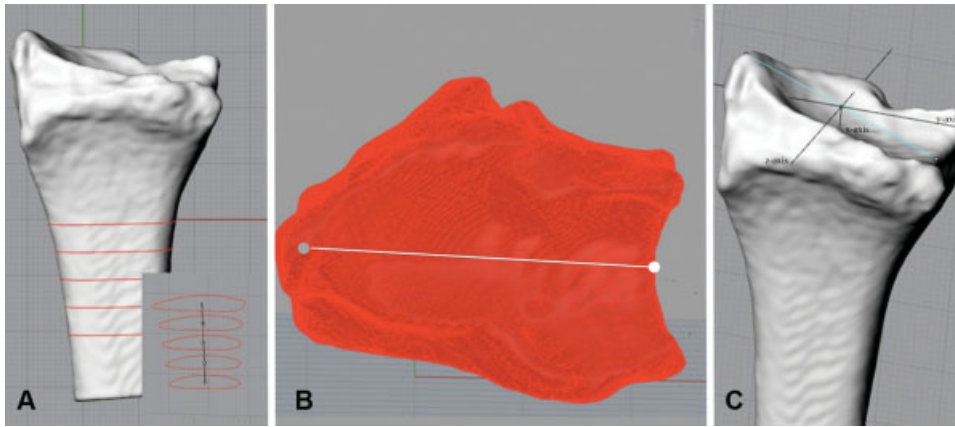


**Fig. 4** The x-axis represents proximal to distal, the y-axis radioulnar, and the z-axis dorsal-to-volar. The x-axis is aligned with the longitudinal axis of the radius as defined by the line through the centroid of the five circumferences along the longitudinal axis of the radial shaft<sup>28,29</sup> (A). The y-axis was from the tip of the radial styloid (gray dot) and the most radial aspect of the ulnar notch (white dot)<sup>29,30</sup> (B). The z-axis resulted from these x- and y-axes (C).

points placed in the centroid of the five circumferences along the longitudinal axis of the radial shaft.<sup>28,29</sup> The circumferences were 0.5 cm proximal from each other, starting 3 cm proximal from the articular surface (►Fig. 4A). The direction of the y-axis was determined by a line through the distal tip of the radial styloid and the most radial aspect of the ulnar notch<sup>29,30</sup> (►Fig. 4B). The z-axis resulted from these x- and y-axes (►Fig. 4C).

#### Relation of RSA-Marked Soft Tissue Landmarks<sup>8,12–15</sup> and Q3DCT-Defined Osseous Landmarks<sup>1–7,17–27</sup>

The following landmarks were quantified using Q3DCT techniques.<sup>10,31</sup> The ulnar and radial prominences were defined as the two most prominent points determined by turning the model around its x-axis and defining the two highest points on the z-axis (►Fig. 5A). The interfossa sulcus<sup>28</sup> was defined as the most dorsal point between the ulnar and radial prominences (►Fig. 5B). A transverse line was drawn between the radial and the ulna prominence, and the point on the watershed line with the greatest distance to the transverse line parallel to the z-axis was determined. A transverse line was drawn between the radial and the ulna prominence, and the point on the watershed line with greatest distance to the transverse line parallel to the z-axis was determined. Two points on the joint line directly distal to the respective radial and ulnar prominences were also marked (►Fig. 5C). The most ulnar point of the volar margin of the distal radius was also verified (►Fig. 5D). Both the identification of all points for the axis-system and all landmarks have been performed by two observers in two specimens, and a 100% agreement on the location for these points was reached.

All measurements were performed parallel to the respective axis using the analyze distance function in rhinoceros and determining the intersection of the two respective lines in a plane parallel to the respective axis (►Fig. 3B). We measured in the proximal to distal direction; the maximum and minimum distances between the marked watershed line and the distal border of the PQ, the distance between bony ulnar and radial prominences and the interfossa sulcus and the PQ (►Fig. 6A) and the distance between the joint line and

the true ulnar and radial prominences and between the radial and ulnar prominence and the interfossa sulcus themselves (►Fig. 6B). The most radial coordinate of the PQ was used to determine the distance between the PQ and the radial prominence. The joint line was defined as the knuckle line of the distal volar radius using the “vertex” function in “shaded” mode in a view perpendicular to the x-axis. We measured in the ulnar to radial direction; the distance between the ulnar prominence, interfossa sulcus, and the ulnar border of the distal radius (►Fig. 6C). We measured in anterior–posterior direction; the distance between the ulnar prominence, radial prominence, and the interfossa sulcus (►Fig. 6D).

#### Mapping of the Watershed Line and the Pronator Quadratus

According to the mapping technique as described by Cole et al<sup>32,33</sup> and modified by our group,<sup>9,11</sup> in this study the distal border of the PQ rather than a fracture line distribution and location were determined using Q3DCT techniques. Images of the 3D polygon mesh were obtained and imported in Macromedia Fireworks MX (Macromedia Inc., San Francisco, CA) to create bitmap images. These bitmap images were superimposed onto a distal radius template to form a compilation of distribution of the watershed line and the PQ. ►Figure 7 demonstrates the template of the radius, and mapping of the watershed line and the PQ of all specimens.

#### Statistical Analysis

Specimen characteristics were summarized with frequencies and percentages for categorical variables and with mean and standard deviation for continuous variables.

## Results

### Watershed Line in Reference to Osseous Anatomy<sup>1–7,17–27</sup>

In the proximal-to-distal direction, on the x-axis, the radial prominence was situated proximal to the joint line of the

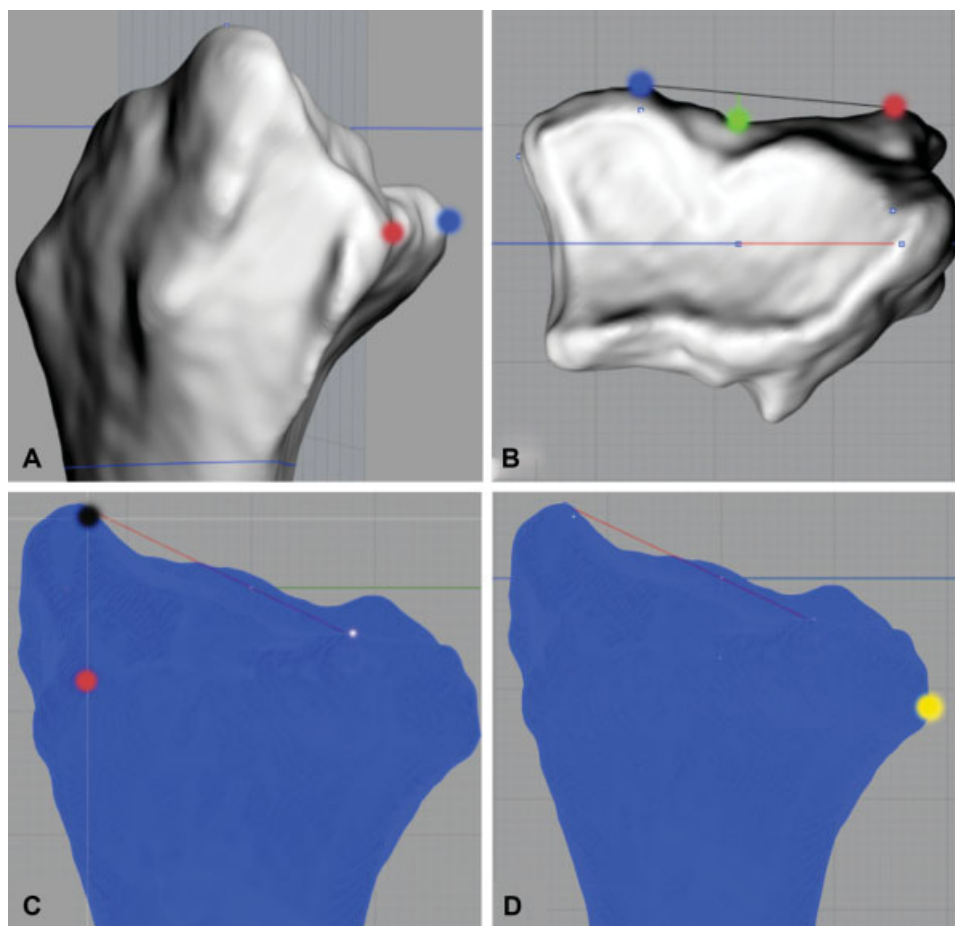


**Fig. 5** Distal radius landmarks<sup>10,31</sup>: (A) The ulnar and radial prominences are the two most prominent volar points. (B) The bone of the interfovea sulcus<sup>28</sup> was defined by drawing a line between the ulnar and radial prominence and determining the point of the volar margin of the distal radius that was furthest away from this line. (C) The point on the joint line directly distal to the radial prominence was defined using the vertex and intersection functions. (D) In anteroposterior view, perpendicular to the x-axis, the most ulnar point of the volar margin of the distal radius was marked.

scaphoid facet of the distal radius in eight specimens. In two specimens, this measurement could not be performed as the radial prominence was located more radial than the joint line, but more radial. The mean distance between the ulnar prominence and the joint line of the lunate facet was far less than between the radial prominence and the proximal joint line of the scaphoid facet (mean 2.1 vs. 11.1 mm) (►Table 1, ►Fig. 6B).

The radial prominence is located proximal compared to the ulnar prominence. The interfovea sulcus was located proximal to the ulnar prominence in six specimens. In the other four specimens, the interfovea sulcus was situated distal to the ulnar prominence. The radial prominence was situated proximal to the interfovea sulcus (►Fig. 6B).

In the ulnar-to-radial direction, on the y-axis, the interfovea sulcus was located between the ulnar and the radial prominence, on average slightly more toward the ulnar prominence. (►Table 2, ►Fig. 6C).

On average, in the volar-to-dorsal direction (z-axis), the interfovea sulcus was located between the ulnar and the radial prominence. In all specimens, the interfovea sulcus was dorsal to the ulnar prominence. In eight specimens, the interfovea sulcus was volar to the radial prominence. In two specimens,

the interfovea sulcus was dorsal to the radial prominence (►Table 3, ►Fig. 6D).

#### Watershed Line Defined in Reference to Soft Tissue Anatomy<sup>8,12-15</sup>

The distances between the distal border of the PQ and the watershed line varied widely. In two specimens, the radial prominence was situated, respectively, 1.3 and 0.2 mm, more proximal to the most radial point of the PQ; in all other specimens, the entire PQ was situated well proximal to the watershed line. The mean minimum distance in distal-to-proximal direction between the watershed line and the PQ was 3.5 mm and the mean maximal distance was 7.6 mm. In all specimens, the distance between the PQ and the watershed line was smaller on the radial side than on the ulnar side.

#### Reference Standard—Three-Dimensional Computed Tomography and Mapping of Pronator Quadratus in Relation to the Watershed line

The distribution and location of the PQ and the watershed line are represented in ►Fig. 7 for all 10 specimens. In all cadaveric specimens, the radial edge of the PQ was situated more ulnar than the level of the radial prominence (►Table 1, ►Fig. 6A).

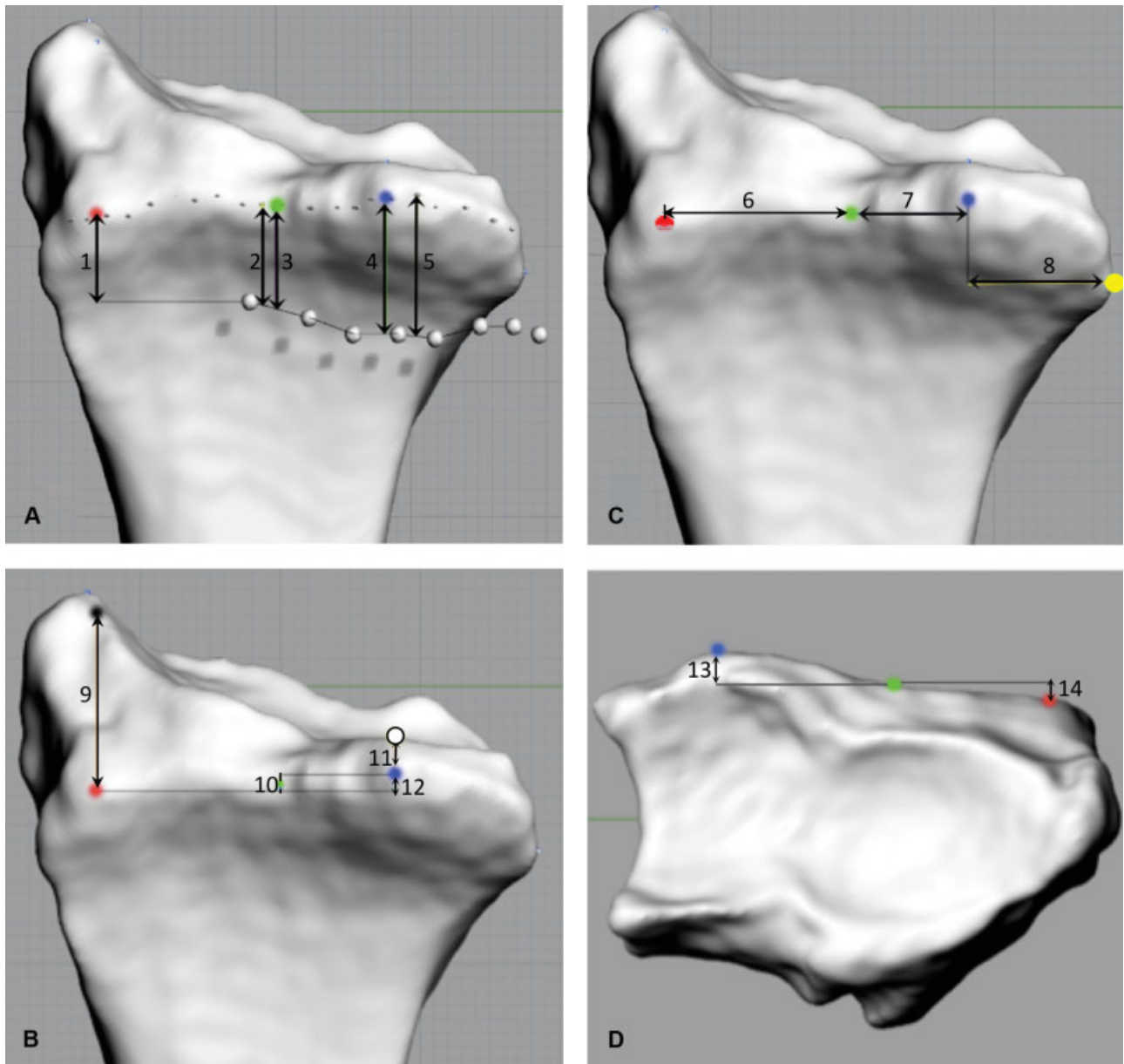


**Fig. 6** Proximal–distal distances soft tissue–osseous anatomy (A) and osseous anatomy (B). Ulnar–radial distances (C). Volar–dorsal distances (D). 1. Radial prominence–PQ 2. Min. Watershed–PQ 3. Interfossa sulcus–PQ 4. Ulnar prominence–PQ 5. Max. Watershed–PQ 6. Sulcus–radial prominence 7. Ulnar prominence–sulcus 8. Ulnar notch–ulnar prominence 9. Joint line–radial prominence 10. Ulnar prominence–sulcus 11. Joint line–Ulnar prominence 12. Ulnar prominence–Radial prominence 13. Ulnar prominence–Sulcus. 14. Sulcus–radial prominence.

## Discussion

The aim of this study was to identify available intra-operative macroscopic anatomical landmarks that can be utilized by orthopaedic surgeons during volar plating for distal radius fractures and relate these to the osseous watershed line using Q3DCT as a reference to optimize volar plate application.

The results of this study should be interpreted in the light of its strengths and weaknesses. A major strength of the study is its newly designed method of identifying anatomical landmarks that allow for relating these landmarks to the osseous watershed line in intact cadaveric wrists following the FCR approach using Q3DCT imaging techniques. A weak-

ness of this study is that it is performed on intact distal radii without them being distorted by a fracture.

The results show that the watershed line, including the volar radial and especially ulnar osseous prominences, is situated well distal to the insertion of the PQ. Additionally, the ranges of distances between the watershed line and soft tissue anatomy (i.e., PQ) varied widely, indicating there is a large variability between individuals. Additionally, the PQ is oriented more ulnar than the watershed line, and using the PQ as reference might result into ulnar placement of a volar plate. In concordance to Orbay's description of the watershed line,<sup>1</sup> this line is situated between 10 and 15 mm proximal to the joint line on the radial side and 2 mm proximal to the joint line on the ulnar side. We found the radial prominence

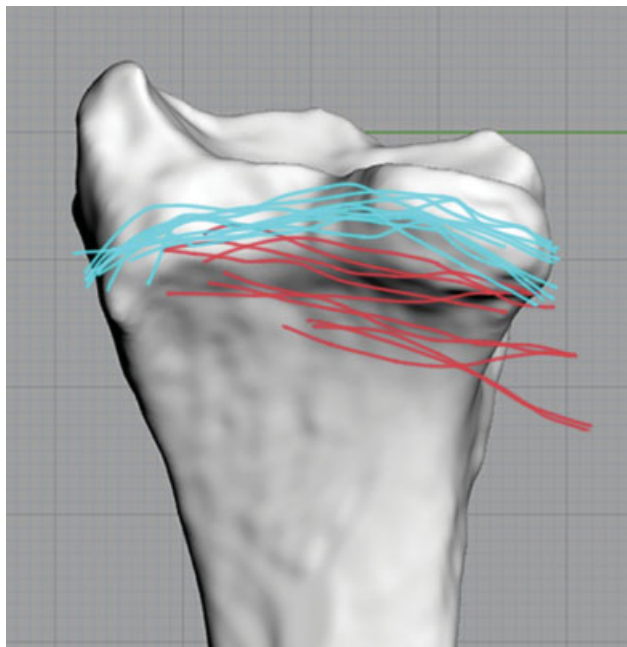


**Fig. 7** Distal radius with mapping of the watershed line (light lines) and the pronator quadratus (PQ) (dark lines) of all 10 specimens. Note the wide range, which makes the PQ position an unreliable surgical reference.

**Table 1** Distal-to-proximal distances (x-axis, ►Fig. 6B)

Distance between	Mean (mm)	Range (mm)
Osseous anatomy		
Joint line of scaphoid facet—radial prominence <sup>a</sup>	11.1	6.6–13.5
Joint line of lunate face—ulnar prominence	2.1	1.3–3.5
Ulnar prominence—radial prominence	2.0	0.5–4.7
Ulnar prominence—interfossa sulcus (in 6 specimens)	1.2	–0.1–3.2
Interfossa sulcus—ulnar prominence (in 4 specimens)	1.0	0.2–1.7
Interfossa sulcus—radial prominence	1.4	0.1–3.7
Soft tissue—osseous anatomy		
Minimum distance watershed line—PQ	3.5	1.2–7.2
Maximum distance watershed line—PQ	7.6	3.6–10.6
Ulnar prominence—PQ	7.2	2.3–10.0
Radial prominence—PQ	2.8	–1.3–0.5 <sup>b</sup>
Interfossa sulcus—PQ	4.8	1.7–7.4

Abbreviation: PQ, pronator quadratus.

<sup>a</sup>Measurement performed in eight specimens, as in two specimens the radial prominence was located more radially than the radial border of the joint line.

<sup>b</sup>Including two specimens in which the radial prominence was situated respectively 0.2 and 1.3 mm more proximal than the most radial point of the PQ (expressed in a negative value).

is indeed on average 11.1 mm and the ulnar prominence on average 2.1 mm proximal to the joint line. As the ulnar prominence is easy to identify by palpation with the overlying fibrous transition zone, we would recommend this

**Table 2** Ulnar-to-radial distances (y-axis, ►Fig. 6C)

Distance between	Mean (mm)	Range (mm)
Ulnar notch—ulnar prominence	8.3	7.0–13.0
Ulnar prominence—interfossa sulcus	9.7	5.0–13.7
Ulnar notch—interfossa sulcus	18.2	12.1–21.9

**Table 3** Volar-to-dorsal distances (z-axis, ►Fig. 6D)

Distance between	Mean (mm)	Range (mm)
Ulnar prominence—interfossa sulcus	3	1.8–5.6
Interfossa sulcus—radial prominence (in 8 specimens)	1.2	0.3–2.1
Radial prominence—interfossa sulcus (in 2 specimens)	0.8	0.4–1.2

osseous ulnar prominence as the most useful anatomical reference in clinical practice for correct volar plate positioning. Fluoroscopic images could easily further aid to identification of the ulnar prominence. Further research can be conducted on the relation of different volar plates to the watershed line and described anatomical landmarks.

The ulnar prominence, defined as “most volar extend on the volar rim ...of the distal radius,” has also been used as reference point for safe plate positioning on radiological imaging,<sup>5</sup> as suggested in a previous anatomical study of the volar surface of the distal radius.<sup>6</sup> In this study, we have described how this point is related to other anatomical references involved in distal radius fracture surgery. The ulnar prominence is on average located 7.2 mm distal to the distal border of the PQ and 8.3 mm radial from the ulnar notch. However, while placing the volar plate one should keep in mind the radial prominence, another relevant point situated on the watershed line is located on average 2.0 mm more proximal than the ulnar prominence.

Another important point on the watershed line is arguably the interfossa sulcus, where the FPL may glide over a plate and cause FPL rupture.<sup>28</sup> As the interfossa sulcus was on average situated only 0.3 mm proximal from the ulnar prominence, the ulnar prominence indeed seems to be a relevant reference point for the watershed line. The interfossa sulcus was located distal to the radial prominence in all cadaveric specimens analyzed in this study, with a mean of 1.4 mm. In most specimens, the interfossa sulcus was located proximal to the ulnar prominence.

## Conclusion

For safe placement of the volar plate for distal radius fractures, the surgeon needs easily identifiable landmarks. The insertion of the PQ is situated well proximal from the watershed line and orientated more ulnarly. The osseous ulnar prominence is a good anatomical reference point for

the watershed line, as it is located on the watershed line and easily palpated upon surgery. We argue that the ulnar prominence could be used as the “Watershed Point” to refer to the watershed line in clinical practice, as it is easy identifiable upon palpation. While using this anatomical reference point, one should keep in mind the sulcus, which is arguably the most important point on the watershed line, can be situated just proximal from the ulnar prominence.

#### Conflict of Interest

None declared.

#### References

- Orbay J. Volar plate fixation of distal radius fractures. *Hand Clin* 2005;21(03):347–354
- Orbay JL, Touhami A. Current concepts in volar fixed-angle fixation of unstable distal radius fractures. *Clin Orthop Relat Res* 2006;445(445):58–67
- Nelson DL, Orbay J, Bindra R. Anatomy of the Volar Distal Radius. 2008 <http://eradius.com/AnatomyOfDistalRadius.htm>
- Arora R, Lutz M, Hennerbichler A, Krappinger D, Espen D, Gabl M. Complications following internal fixation of unstable distal radius fracture with a palmar locking-plate. *J Orthop Trauma* 2007;21(05):316–322
- Soong M, Earp BE, Bishop G, Leung A, Blazar P. Volar locking plate implant prominence and flexor tendon rupture. *J Bone Joint Surg Am* 2011;93(04):328–335
- Imatani J, Akita K, Yamaguchi K, Shimizu H, Kondou H, Ozaki T. An anatomical study of the watershed line on the volar, distal aspect of the radius: implications for plate placement and avoidance of tendon ruptures. *J Hand Surg Am* 2012;37(08):1550–1554
- Obert L, Loisel F, Gasse N, Lepage D. Distal radius anatomy applied to the treatment of wrist fractures by plate: a review of recent literature. *SICOT J* 2015;1:14
- Agnew SP, Ljungquist KL, Huang JI. Danger zones for flexor tendons in volar plating of distal radius fractures. *J Hand Surg Am* 2015;40(06):1102–1105
- Mellema JJ, Doornberg JN, Dyer GS, Ring D. Distribution of coronoid fracture lines by specific patterns of traumatic elbow instability. *J Hand Surg Am* 2014;39(10):2041–2046
- de Muinck Keizer RO, Meijer DT, van der Gronde BA, et al. Articular gap and step-off revisited: 3D quantification of operative reduction for posterior malleolar fragments. *J Orthop Trauma* 2016;30(12):670–675
- Molenaars RJ, Mellema JJ, Doornberg JN, Kloen P. Tibial plateau fracture characteristics: computed tomography mapping of lateral, medial, and bicondylar fractures. *J Bone Joint Surg Am* 2015;97(18):1512–1520
- Ahsan ZS, Yao J. The importance of pronator quadratus repair in the treatment of distal radius fractures with volar plating. *Hand (N Y)* 2012;7(03):276–280
- Goorens CK, Van Royen K, Grijseels S, et al. Ultrasonographic evaluation of the distance between the flexor pollicis longus tendon and volar prominence of the plate as a function of volar plate positioning and pronator quadratus repair - A cadaver study. *Hand Surg Rehabil* 2018;37(03):171–174
- Kara A, Celik H, Bankaoglu M, Oc Y, Bulbul M, Sugun TS. Ultrasonic evaluation of the flexor pollicis longus tendon following volar plate fixation for distal radius fractures. *J Hand Surg Am* 2016;41(03):374–380
- Singh TS, Sadagatullah AN, Yusof AH. Morphology of distal radius curvatures: a CT-based study on the Malaysian Malay population. *Singapore Med J* 2015;56(10):562–566
- Orbay JL. The treatment of unstable distal radius fractures with volar fixation. *Hand Surg* 2000;5(02):103–112
- Rajeev AS, Sreerethana S, Harrison J. Rupture of flexor pollicis longus tendon: a complication of volar locking plating of the distal radius. *Eur J Trauma Emerg Surg* 2010;36(04):385–387
- Valbuena SE, Cogswell LK, Baraziol R, Valenti P. Rupture of flexor tendon following volar plate of distal radius fracture. Report of five cases. *Chir Main* 2010;29(02):109–113
- McCann PA, Amirfeyz R, Wakeley C, Bhatia R. The volar anatomy of the distal radius—an MRI study of the FCR approach. *Injury* 2010;41(10):1012–1014
- McCann PA, Clarke D, Amirfeyz R, Bhatia R. The cadaveric anatomy of the distal radius: implications for the use of volar plates. *Ann R Coll Surg Engl* 2012;94(02):116–120
- Adham MN, Porembski M, Adham C. Flexor tendon problems after volar plate fixation of distal radius fractures. *Hand (N Y)* 2009;4(04):406–409
- Buzzell JE, Weikert DR, Watson JT, Lee DH. Precontoured fixed-angle volar distal radius plates: a comparison of anatomic fit. *J Hand Surg Am* 2008;33(07):1144–1152
- Im JH, Lee JY. Pearls and pitfalls of the volar locking plating for distal radius fractures. *J Hand Surg Asian Pac Vol* 2016;21(02):125–132
- Tanaka Y, Aoki M, Izumi T, Fujimiya M, Yamashita T, Imai T. Effect of distal radius volar plate position on contact pressure between the flexor pollicis longus tendon and the distal plate edge. *J Hand Surg Am* 2011;36(11):1790–1797
- Wilson J, Viner JJ, Johal KS, Woodruff MJ. Volar locking plate fixations for displaced distal radius fractures: an evaluation of complications and radiographic outcomes. *Hand (N Y)* 2018;13(04):466–472
- Oppermann J, Wacker M, Stein G, et al. Anatomical fit of seven different palmar distal radius plates. *Arch Orthop Trauma Surg* 2014;134(10):1483–1489
- Imatani J, Akita K. Volar distal radius anatomy applied to the treatment of distal radius fracture. *J Wrist Surg* 2017;6(03):174–177
- Limthongthang R, Bachoura A, Jacoby SM, Osterman AL. Distal radius volar locking plate design and associated vulnerability of the flexor pollicis longus. *J Hand Surg Am* 2014;39(05):852–860
- Oura K, Oka K, Kawanishi Y, Sugamoto K, Yoshikawa H, Murase T. Volar morphology of the distal radius in axial planes: a quantitative analysis. *J Orthop Res* 2015;33(04):496–503
- Schwarz Y, Schwarcz Y, Peleg E, Joskowicz L, Wollstein R, Luria S. Three-dimensional analysis of acute scaphoid fracture displacement: proximal extension deformity of the scaphoid. *J Bone Joint Surg Am* 2017;99(02):141–149
- Bexkens R, Oosterhoff JH, Tsai TY, et al. Osteochondritis dissecans of the capitellum: lesion size and pattern analysis using quantitative 3-dimensional computed tomography and mapping technique. *J Shoulder Elbow Surg* 2017;26(09):1629–1635
- Armitage BM, Wijdicks CA, Tarkin IS, et al. Mapping of scapular fractures with three-dimensional computed tomography. *J Bone Joint Surg Am* 2009;91(09):2222–2228
- Cole PA, Mehrle RK, Bhandari M, Zlowodzki M. The pilon map: fracture lines and comminution zones in OTA/AO type 43C3 pilon fractures. *J Orthop Trauma* 2013;27(07):e152–e156